MATERIAL FIRE PROPERTIES

J. G. Quintiere, J. Torero, R. T. Long[1], S. E. Dillon[2], N. Wu[3] and D. Heater
Department of Fire Protection Engineering
University of Maryland
College Park, MD 20742

ABSTRACT

A description of fire properties is presented for common material products in terms of measurement methodology and their theoretical interpretation. Properties related to phenomena of ignition , flame spread, and burning rate are discussed. The properties include: thermal inertia, ignition temperature, heat of combustion, heat of gasification, total energy and opposed flow flame spread properties. An illustration of the importance of the properties in predicting fire growth is presented in a correlation of flashover time for the ISO 9705 room-corner test. The correlation shows a sharp threshold for flashover in terms of a correlating variable involving several properties related to upward flame spread.

INTRODUCTION

The ability to predict the performance of materials and products in fire requires models that can accurately represent the phenomenon, and measured properties of the material consistent with the models. Since most products, and even pure materials, display many physical and chemical changes in their degradation in fire, it is not practical to represent all of these effects in terms of fundamental processes and properties. The art of making successful predictions is to capture the key effects, and incorporate them into measurable properties and models that have universality and consistency. Other implicit effects ignored would then be swept into the properties. The properties to be considered might be regarded as pseudo-properties since they may characterize several phenomena, as distinct from well defined thermodynamic and transport properties.

Tewarson (1988) has systematically shown how fire properties of materials can be measured in order to describe their evolution of smoke and energy under different fire conditions. Quintiere and Harkleroad (1984) have shown how measurements could be practically performed to characterize useful flame spread and ignition properties. Standard test apparatuses can be used to make these measurements; namely, the Factory mutual Flammability Apparatus (Tewarson, 1988), the Cone Calorimeter (ASTM E 1354), and the LIFT device (ASTM E 1321). However, the property measurements should not be apparatus dependent, and other comparable devices should be just as appropriate for making the measurements. Indeed, for some of the data presented here, the Roland apparatus developed by the LSF Laboratories (Su, 1997) was used as a larger version of the LIFT, and a smaller version was also used in a study for NASA (Long, 1998).

---

[1] Currently with Exponent Failure Analysis Assoc.

[2] Southwest Research Institute

[3] Rolf Jensen and Assoc.

This paper will illustrate the theory and measurement bases for the interpretation of material fire properties associated with fire growth. It will address ignition, burning rate and energy release, and flame spread. Illustrations will be given from recent property determinations made in our laboratory in cooperation with the LSF Laboratories of Italy and the Building Research Institute of Japan, who supplied the raw data; and from studies supported by NIST and NASA. These results should indicate the scope of the application since a diverse range of materials have been considered. A theoretical basis for the property measurement will be presented along with some representative results. An example of the use of properties in predicting fire growth will be given in terms of a correlation, based on upward flame spread, to predict flashover times in the ISO 9705 room-corner test.

IGNITION

The simplest theory for the ignition of solids is based on pure conduction without degradation of the solid, and on the concept of a fixed ignition temperature, T_{ig}. The ignition temperature is equivalent to the flashpoint of liquid fuels. The flashpoint corresponds to the surface temperature sufficient to cause an evaporating vapor concentration equal to the lower flammable limit. Hence, on submission of a suitable energy source or pilot flame, this mixture will ignite and propagate. Once a flame occurs, its additional heating of the surface is usually sufficient to cause sustained burning. Since lower flammable limit concentrations are very low, typically 5 % or less, then very little evaporation is needed. Therefore, it is expected that a solid under the same circumstance will require little degradation to cause piloted ignition. Based on the concept of a fixed ignition temperature of a material, an expression can be derived for the time to ignition:

$$t_{ig} = \frac{p}{4} \frac{krc\left(T_{ig} - T_{\infty}\right)^2}{\dot{q}_i''^{\,2}} \qquad (1)$$

where k = thermal conductivity,
ρ= density,
c = specific heat,
T_∞ = initial temperature,
and $\dot{q}_i''$ = incident heat flux.

This equation is approximate and holds only under the following conditions:
(1) the solid is inert and homogeneous,
(2) thermal properties are constant,
(3) its surface emissivity and absorptivity are both unity,
(4) the incident heat flux is much greater than the surface heat losses,
and (5) the solid is very thick.

In the last restriction, usually thicknesses greater than 1 mm are sufficient or the effective thickness can be considered to be composed of the combustible material and its substrate. An example of the latter condition is paint or wall paper on gypsum board. The restriction by (1) appears to be reasonable as long as the time to a phase change or significant decomposition is long compared to the subsequent time to achieve a flammable gaseous mixture.

The applicability of this ignition model is judged by how well it can represent data. Figure 1 shows that $t^{-1/2}$ is linear in $\dot{q}_i''$ as Eq. (1) predicts. These data from Long (1998) are for radiative ignition of vertical black polymethylmethacrylate (PMMA) in sample heights ranging from 35 to 155 mm. At a low enough heat flux the material can never reach its ignition temperature. Ideally for an inert material, the lowest heat flux to cause ignition must equal the surface heat losses. This can be expressed as

$$\dot{q}''_{i,crit} = h(T_{ig} - T_\infty) \qquad (2)$$

where h represents an overall heat transfer coefficient involving convection and radiation. Not

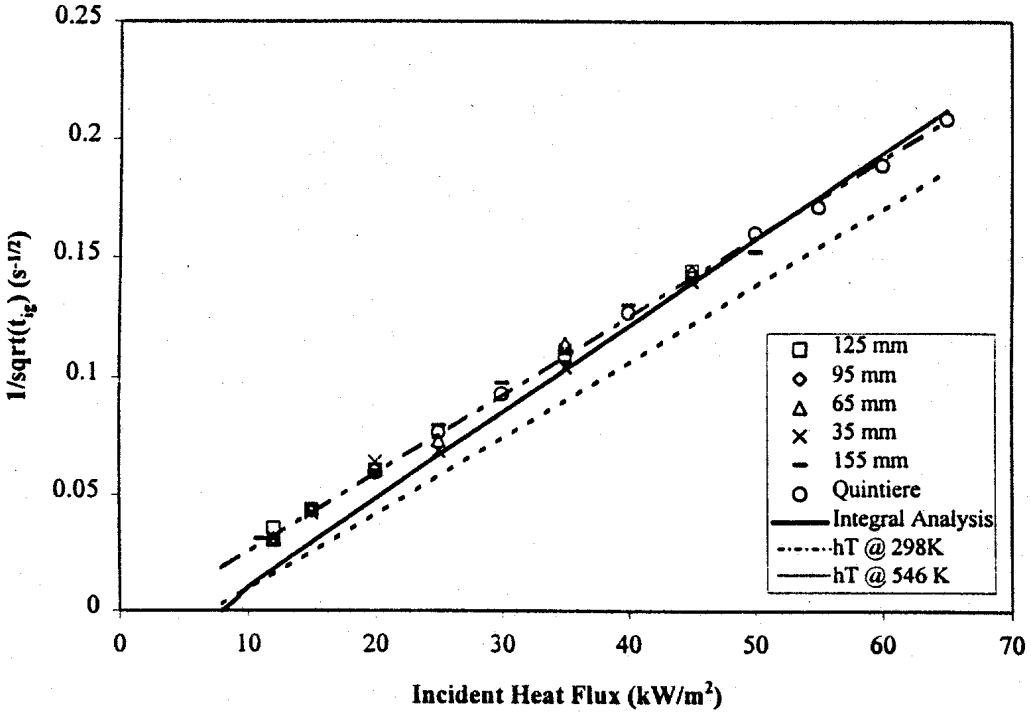

Figure 1. Radiative piloted ignition for PMMA from Long (1998)

shown in Figure 1 is a critical heat flux of 11 kW/m^2 at which ignition does not occur. From this value and being able to represent h as a function of temperature, T_{ig} can be determined. Once this is known, the thermal property kρc can be determined from the slope of the data in Figure 1. This methodology is expressed in the LIFT (ASTM E 1321) standard and allows a deduction of the material fire properties : T_{ig} and kρc.

From the approximation in the ignition model, it should be clear that these are really modeling properties. However, they do have physical and chemical significance. In general, it should be realized that k and c usually increase with temperature, and k is proportional to density in solids. Furthermore, as a solid melts or decomposes, the endothermisity of the these processes should yield an increase in this effective kρc property. Adding an inert chemical which decomposes before ignition, such as one that releases water, would both increase kρc and increase T_{ig} since both endothermisity and dilution of the gaseous fuel mixture would occur. A similar effect should occur for a flame inhibiting agent. A thin material on a high density noncombustible substrate would tend to represent more the kρc property of the substrate while reflecting an ignition temperature of the thin material.

The method for deducing the ignition temperature from critical flux ignition data is approximate. Yet in a study by Wu (1998) of the radiant ignition of weathered crude oils in forced convection, a distinct linear relationship was found to exist between measured flashpoint temperature and

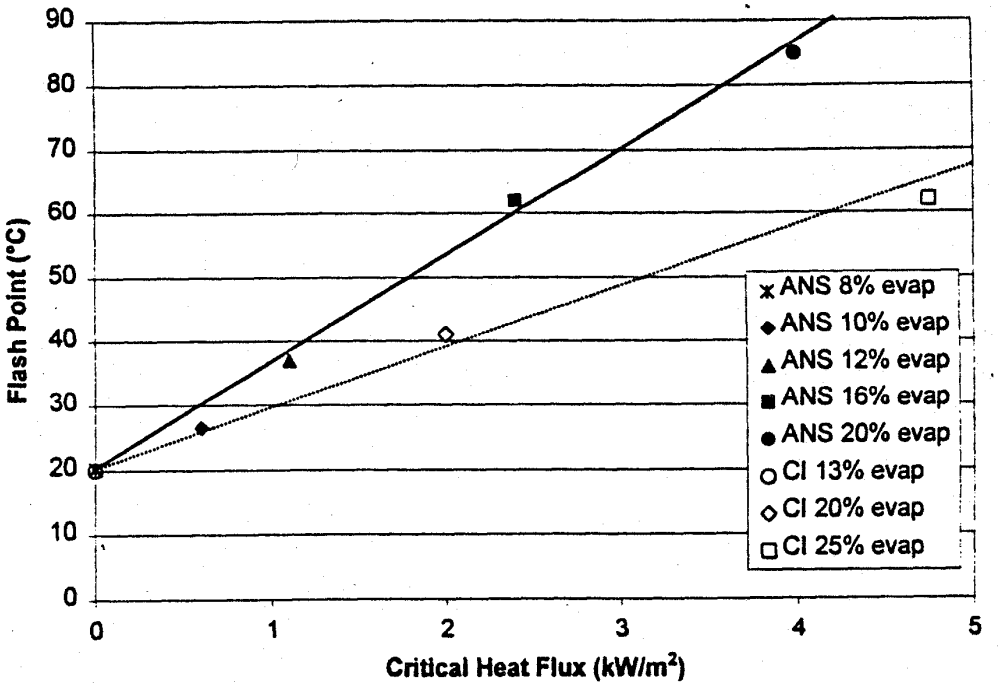

Figure 2. Flashpoint as a function of critical heat flux in weathered crude oils (Wu, 1998)

estimated critical heat flux for each of the weathered samples. This is shown in Figure 2. It appears that the two crude oils, ANS and Cook Inlet, have different absorptivities which would explain the two lines instead of a unique relationship between ignition temperature and critical flux as given by Eq. (2). Hence, a derivation of ignition temperature by Eq. (2) can only yield a relative temperature which fits the modeling assumptions.

OPPOSED FLOW FLAME SPREAD

Flame spread is related to ignition such that to maintain spread, the material ahead of the burning region must continually be brought to its ignition temperature. For the case of flame spread into a wind or into a naturally induced buoyant flow in downward or lateral spread, the flame is directed away for the material seeking to be ignited. For such spread, the flame configuration usually remains constant and the spread rate remains steady. For practical applications to real materials, it has been found useful to express the spread velocity (V) as

$$V = \frac{\Phi}{krc(T_{ig} - T_s)^2} \qquad (3)$$

This has been found to hold for T_s, the surface temperature before flame heating, above a minimum value. This minimum temperature has been found to be material dependent. The parameter Φ is a complex function involving flame heat transfer, the speed of the air flow opposing the spread, and chemical kinetics. Despite these dependencies, Φ can be determined from testing to be an approximate material property over limited conditions. In testing, Φ is derived from tests in which radiant heating is distributed over the sample so that a known incident heat flux produces a corresponding surface temperature, T_s. From a relationship like Eq. (2), Ts can inferred in the same way as T_{ig}.

A standard test for this procedure is the LIFT apparatus (ASTM E 1321), but variations have been executed with the Roland apparatus by Su (1997) for both downward and lateral spread, and for horizontal spread on crude oil by Wu (1998). Results plotted in terms of the incident heat flux give $V^{-1/2}$ linear with $\dot{q}''_{i,crit} - \dot{q}''_i$ as long as h can be regarded as a constant in relating surface temperature rise to heat flux as given by Eq. (2). For the same PMMA material discussed in Figure 1 for ignition, Long (1998) displays results for lateral flame spread (Figure 3). The linearity of the results appear to hold over the core range of heat flux, but diverge from linearity near the low flux limit. An extrapolation of the line to the zero intercept yield a critical flux for ignition of 12 kW/m^2 which is consistent with 11 kW/m^2 independently estimated from ignition tests.

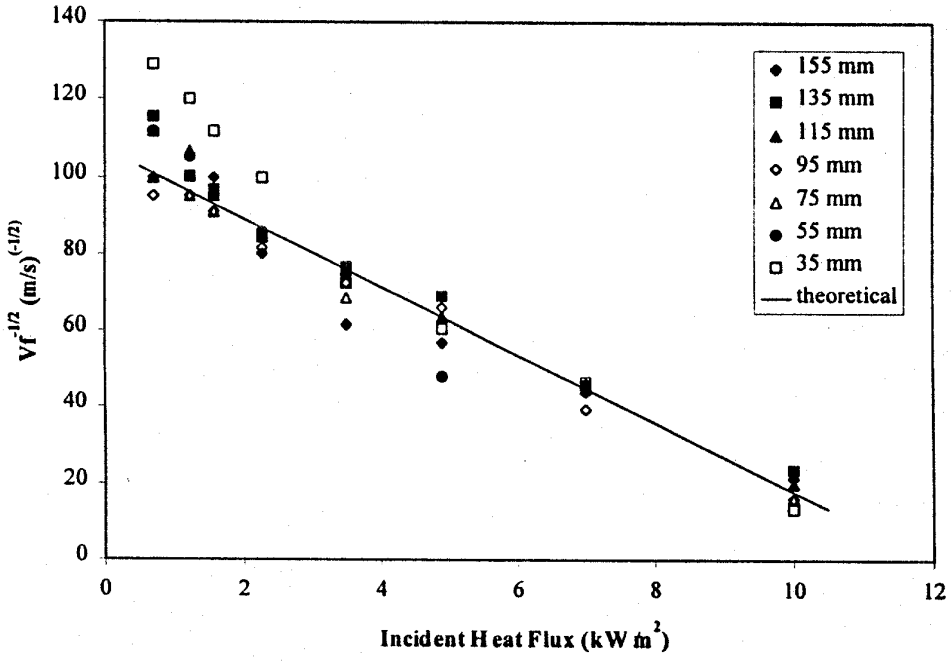

Figure 3. Lateral flame spread on PMMA from Long (1998)

BURNING RATE PER UNIT AREA

The simplest way to describe the burning rate per unit area ($\dot{m}''$) for a material is

$$\dot{m}'' = \dot{q}'' / L \qquad (4)$$

where $\dot{q}''$ is the net heat flux at the surface from the gas phase, and L is the heat of gasification. For the steady burning of a deep pool of liquid fuel in a perfectly insulated container, L is a pure thermodynamic property. It is the sum of the heat of vaporization at approximately the boiling point, and the sensible energy or enthalpy change to bring the fuel from its original temperature to its boiling point. For all other conditions, Eq. (4) is an approximation. For example, in applying Eq. (4) to the burning of solids whose decomposition do not follow thermodynamic behavior, and where charring and heat losses lead to unsteady burning, it must be regarded as approximate. Yet by using controlled conditions of heat flux, it is possible to deduce values for L from data. Such L values can then serve as effective material properties, especially in the application of Eq. (4) to arbitrary heating conditions.

The Cone Calorimeter (ASTM E 1324) is a device in which controlled heating conditions can be achieved. In that device the material would experience a net surface heat flux:

$$\dot{q}'' = \dot{q}_f'' + \dot{q}_{ext}'' - \dot{q}_{rr}'' \qquad (5)$$

where $\dot{q}_f''$ is the flame heat flux,

$\dot{q}_{ext}''$ is the controlled external radiant heat flux,

and $\dot{q}_{rr}''$ is the surface re-radiation heat flux.

It has been shown by Rhodes and Quintiere (1996) that for flame heights greater than about 20 cm in the Cone, the flame heat flux for a given fuel remains nearly constant. This appears due to the radiant feat transfer nature of the characteristic tall column-like flame in the system. Yet the small flame diameter of less than 9 cm allows the flame to be mostly transparent to the imposed radiant heat flux. The re-radiation heat flux will depend on surface temperature and emissivity and these properties can not easily be determined. However, they tend to be close to unity for the heating conditions of the Cone, and therefore it is expedient to take

$$\dot{q}_{rr}'' = s T_{ig}^4 . \qquad (6)$$

Thus, Eqns. (4) - (6) provided a basis for defining L; however, the transient nature of the combustion of solids must still be considered.

Dillon (1998) has examined several procedures for deriving values of L and favors its evaluation at the average peak energy release rate. This has been specifically defined as the average of the energy release rate per unit area, $\dot{Q}''$, taken over the period where it is greater than 80 % of its absolute peak. Figure 4 shows the "peak average" value found by this method along with alternatives of using the absolute peak and an overall value based on the entire flaming period. The results in Figure 4 are for a three-layered box-like structure made of polycarbonate. The "peak average" approach can be misleading when the burning pattern is more complex as for plywood shown in Figure 5. There the magnitude of the first peak can be subject to inaccuracy due to its sharp nature, and the second peak can be more significant to the fire growth process.

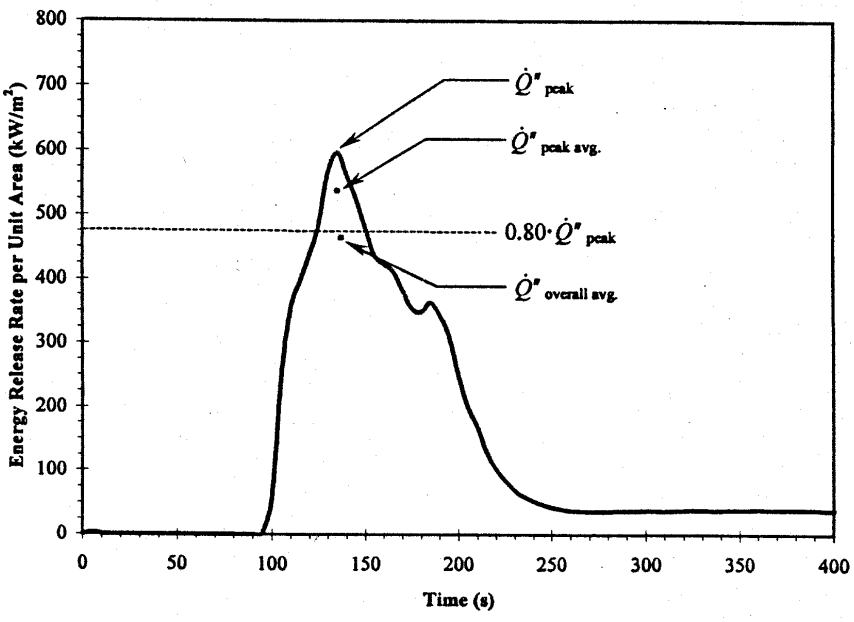

Figure 4. Energy release rate for a polycarbonate box structure at 50 kW/m^2 (Dillon, 1998)

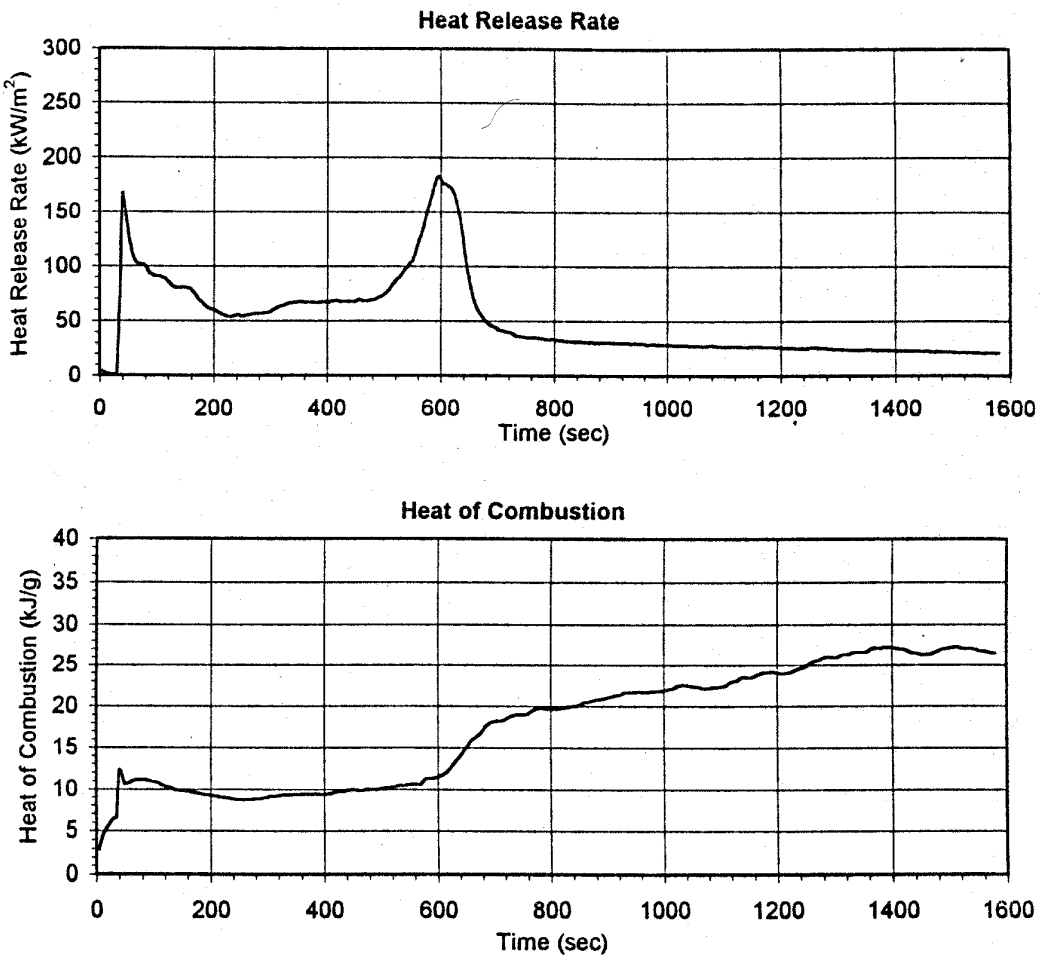

Figure 5. Energy release rate and heat of combustion of plywood at 35 kW/m^2 (Dillon, 1998)

The energy release is related to the burning rate by the heat of combustion, ΔH_c,

$$\dot{Q}'' = \dot{m}'' \Delta H_c . \qquad (7)$$

In the Cone Calorimeter, the heat of combustion is dynamically determined from the instantaneous measurements of energy release and mass loss rates. Figure 5 shows how the heat of combustion varies over time with a value of mostly about 10 kJ/g over the flaming period bounded by the two peaks in the energy release rate curve, and attaining about 25 kJ/g for most of the subsequent char oxidation period.

In the material properties considered in this paper, the values of L and ΔH_c have been determine from the peak average energy release periods. Figures 6 and 7 show examples of the determination of these properties by the peak average method and alternative methods.

Another important property to characterize the combustion of a material is the total burnable fuel available. This is an approximate constant, especially over the flaming phase of combustion. It is represented by Q" determined from the energy release rate per unit area integrated over time up to a lower limit of 25 kW/m^2 to insure flaming persists. It is found that Q" is not a strong function of heat flux and it can be represented by a single characteristic value for a material as illustrated in Figure 8.

For a known heat flux, the energy release rate can be approximated as a square wave function as illustrated in Figure 9 by knowing the properties: ΔH_c, L, Q" and T_{ig}. The time width of the square wave can be computed by

$$t_b = \frac{Q''}{\dot{q}''(\Delta H_c / L)} \tag{8}$$

which gives the average burnout time of the material.

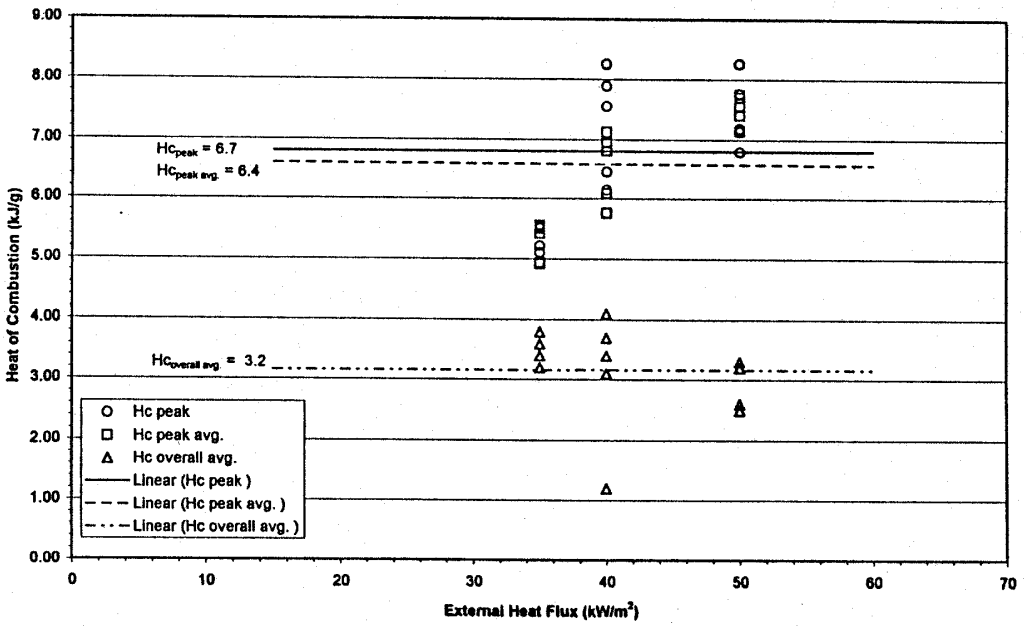

Figure 6. Heat of combustion for paper faced gypsum board from Dillon (1998)

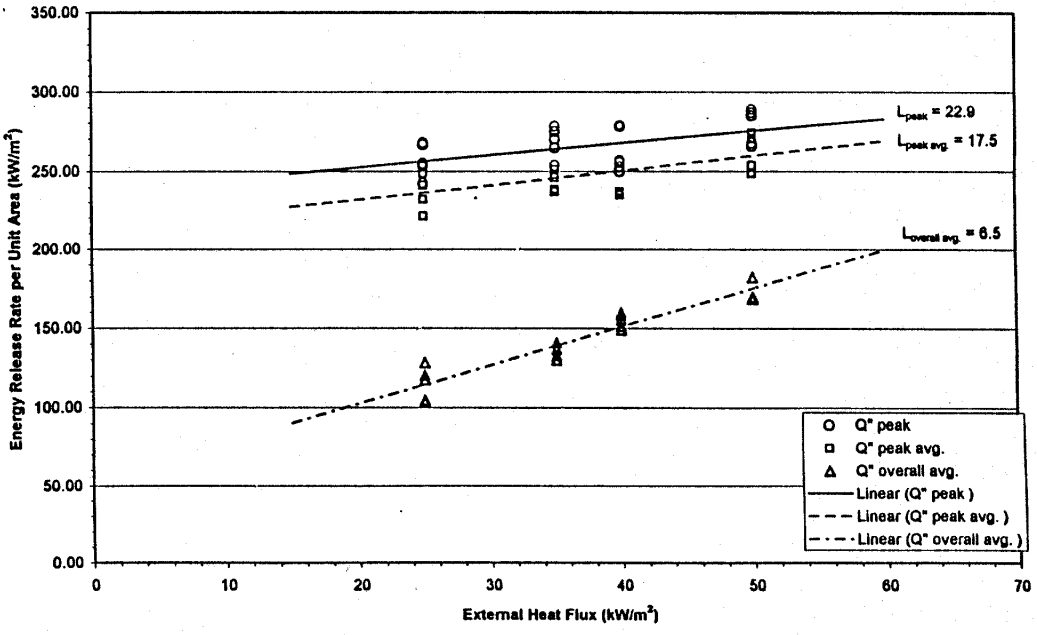

Figure 7. Heat of gasification for varnished timber from Dillon (1998)

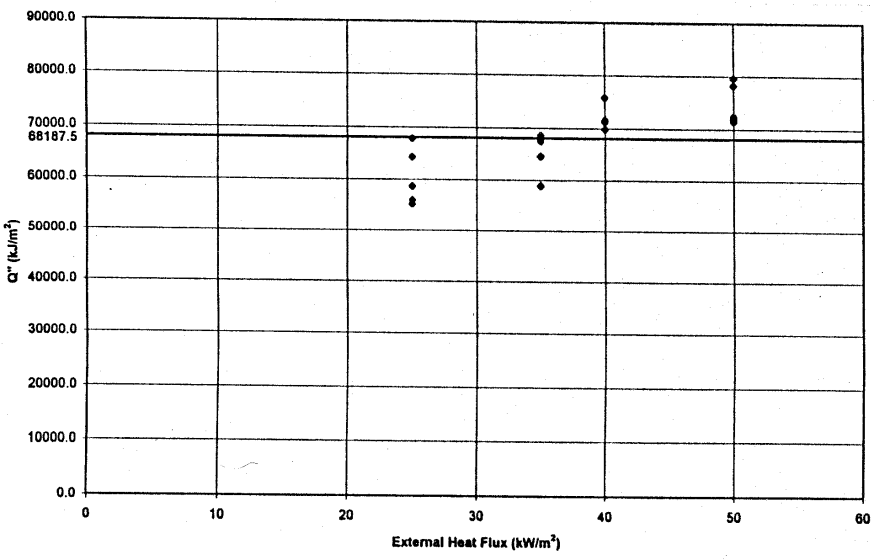

Figure 8. Total energy per unit area of varnished timber from Dillon (1998)

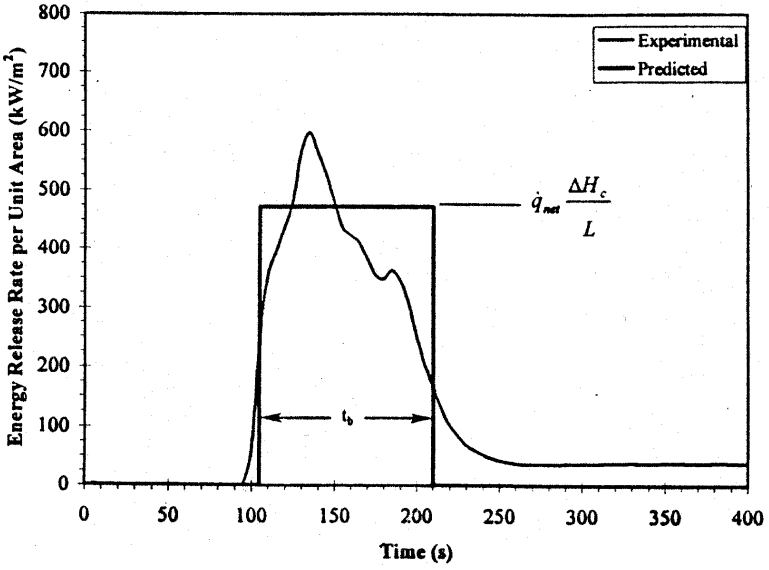

Figure 9. Square wave representation for polycarbonate at 50 kW/m^2 (Dillon, 1998)

UPWARD FLAME SPREAD

In an analysis by Cleary and Quintiere (1991), a solution was found for the rate of growth of the pyrolysis region (Δy) during upward flame spread on a vertical wall. The problem considered the ignition of the region y_o by a flame whose heat flux is the same as the spreading fire. Burnout was also considered so that after burnout the ignition flame over the region y_o no longer contributes to the flame length originating from the pyrolysis region, since y_o is no longer burning. A linear relationship was assumed between flame length and energy release rate, $\dot{Q}''\Delta y$. For a fixed width of the upward burning region and for a constant $\dot{Q}''$, the following is found for the energy release

Table 1. Material Fire Properties

Materials Grouped according to Type	Tig (°C)	Ts,min (°C)	kρc (kW^2s / m^4K^2)	Φ (kW^2 / m^3)	$\Delta Hc_{peak\ avg.}$ (kJ / g)	$L_{peak\ avg.}$ (kJ / g)	Q''_{total} (MJ / m^2)
COMPOSITES							
S4 Gypsum Board	469	380	0.515	14	7	4.8	2.8
R402 Paper Faced Gypsum Board	515	517	0.549	0.0	6.4	4.8	2.2
S6 Paper Wall Covering on Gypsum Board	388	300	0.593	0.5	10	4.8	7.2
8-E Surface Treatment on Gypsum board	516	398	0.562	3.2	20.08	3.48	3.8
8-F F.R. Surface Treatment on Gypsum board	516	273	0.694	20.1	16.07	6.44	5.9
7-Ao PVC Wall Paper (300 g/m^2) on Gypsum board	507	422	0.226	1.7	11.03	3.39	3.5
8-L PVC Wall Paper (800 g/m^2) on Gypsum board	394	300	0.453	7.0	12.70	4.00	8.1
E10 PVC Wallcarpet on Gypsum Board	391	367	0.69	8.2	6.5	3.3	11.0
S5 PVC Covering on Gypsum Board	410	300	0.208	25	13	3.7	4.6
8-B Rayon Wall Paper (300 g/m^2) on Gypsum board	394	217	0.843	24.4	17.06	7.34	6.7
S7 Textile Covering on Gypsum Board	406	270	0.570	9	13	1.5	8.3
E3 Textile Covering on Gypsum Board	387	189	0.97	7.7	7.5	3.1	9.5
8-C Emulsion Paint on Gypsum board	649	594	0.462	14.2	17.84	2.08	3.4
8-D Acrylic Enamel on Gypsum board	560	292	0.419	26.2	14.97	5.12	4.0
E1 Painted Gypsum Paper on Plaster Board	551	478	0.73	3.3	4.1	3.6	3.3
S8 Textile Covering on Mineral Wool	391	174	0.183	6	25	2.8	9.3
E5 Plastic faced Steel Sheet on Mineral Wool	582	472	0.60	44	11.0	34.0	2.5
E7 Combustible faced Mineral Wool	354	263	0.11	0.86	11.0	9.2	1.7
PLASTICS PRODUCTS							
R407 F.R. PVC	415	352	1.306	0.2	9.9	10.4	16.1
S10 Expanded Polystyrene (PS)	482	130	0.464	31	28	1.5	32.0
R420 F.R. Expanded Polystyrene Board (40 mm)	295	77	1.594	4.2	27.5	7.3	33.9
R421 F.R. Expanded Polystyrene Board (80 mm)	490	77	0.557	7.1	26.9	12.7	25.5
E11 Extruded Polystyrene Foam	482	354	0.44	11.5	27.0	2.7	20.0
R405 F.R. Extruded Polystyrene Board	275	77	1.983	1.2	27.8	4.7	38.7
S11 Polyurethane Foam (rigid)	393	105	0.031	3	13	3.1	14.0
R404 PU Foam Panel with Paper Facing	250	77	0.199	8.7	18.9	5.5	30.8
E9 Polyurethane Foam on Plastic faced Steel Sheet	494	326	0.60	22	12.0	5.1	17.0
R406 Clear Acrylic Glazing	195	195	2.957	---	24.1	1.6	89.5
8-H F.R. Polyethylene Foam on Metal Plate (Foam side tested)	593	498	0.713	43.5	57.02	12.93	3.8
R408 3-Layed F.R. Polycarbonate Panel	495	167	1.472	0.0	19.5	3.3	58.1
E4 Melamine faced High Density Non-Combustible Board	631	527	0.32	12.7	8.5	3.5	7.0
WOOD PRODUCTS							
R409 Varnished Massive Timber	330	77	0.530	6.9	16.3	17.5	68.2
S12 Wood Panel (Spruce)	389	155	0.569	24	15	6.3	120.0
R411 Normal Plywood	290	147	0.633	2.2	11.9	7.3	64.6
E2 Ordinary Birch Plywood	392	164	0.99	13	11.9	6.2	75.5
R410 F.R. Plywood	480	197	0.105	0.7	11.2	9.3	51.8
7-Q Soft Fiberboard	245	261	0.581	11.4	13.89	6.39	30.7
S2 Medium Density Fiberboard	361	80	0.732	11	14	4.2	100.0
S1 Insulating Fiberboard	381	90	0.229	14	14	4.2	68.0
R401 F.R.Chipboard	505	507	4.024	0.0	9.2	10.0	34.2
S3 Particle Board	405	180	0.626	8	14	5.4	120.0
S9 Melamine Covering on Particle Board	483	435	0.804	1	11	4.8	60.0
S13 Paper Covering on Particle Board	426	250	0.680	13	13	6.5	100.0
E8 F.R. Particle Board	678	678	1.80	---	6.0	4.0	6.0
E6 F.R. Particle Board Type B1	482	482	0.29	---	3.9	1.4	5.5

Table 2. Correlating parameters in flashover for the ISO room corner test

Materials	t_{fo} (sec)	t_{ig} (sec)	t_b (sec)	τ_{fo} (---)	τ_b (---)	a (---)	b (---)
7-Ao PVC Wall Paper (300 g/m2) on Gypsum board	610	47	28	13.04	0.59	0.27	-1.43
7-Q Soft Fiberboard	54	26	253	2.10	9.84	0.22	0.11
8-B Rayon Wall Paper (300 g/m2) on Gypsum board	672	103	59	6.53	0.57	0.13	-1.61
8-C Emulsion Paint on Gypsum Board	∞	160	21	∞	0.13	0.63	-7.02
8-D Acrylic Enamel on Gypsum board	∞	107	42	∞	0.39	-0.04	-2.59
8-E Surface Treatment on Gypsum board	∞	121	17	∞	0.14	1.19	-5.77
8-F F.R. Surface Treatment on Gypsum board	∞	149	62	∞	0.42	-0.05	-2.45
8-H F.R. Polyethylene Foam on Metal Plate (Foam side tested)	∞	204	31	∞	0.15	0.24	-6.42
8-L PVC Wall Paper (800 g/m2) on Gypsum board	834	55	52	15.08	0.95	0.55	-0.51
R401 F.R.Chipboard	∞	234	948	∞	4.05	-0.64	-1.51
R402 Paper Faced Gypsum Board	∞	33	43	∞	1.28	-0.49	-3.21
R403/ R404 PU Foam Panel with Alum. Face (room test) / Paper Face (bench test)	41	2	161	17.72	69.51	0.92	0.86
R405 F.R. Extruded Polystyrene Board	96	28	119	3.38	4.19	2.25	1.30
R406 Clear Acrylic Glazing	141	19	104	7.12	5.24	7.63	6.87
R407 F.R. PVC	∞	47	343	∞	7.3	-0.55	-1.07
R408 3-Layed F.R. Polycarbonate Panel	∞	81	244	∞	3	1.38	0.19
R409 Varnished Massive Timber	107	11	1394	9.41	122.69	-0.51	-0.54
R410 F.R. Plywood	631	5	1029	117.44	191.58	-0.50	-0.52
R411 Normal Plywood	142	10	729	13.92	71.47	-0.11	-0.17
R420 F.R. Expanded Polystyrene Board (40 mm)	87	26	166	3.26	6.23	1.04	0.41
R421 F.R. Expanded Polystyrene Board (80 mm)	∞	30	290	∞	9.65	-0.14	-0.51
S1 Insulating Fiberboard	59	25	413	2.36	16.52	0.65	0.59
S2 Medium Density Fiberboard	131	72	590	1.82	8.2	0.69	0.57
S3 Particle Board	157	79	964	1.99	12.2	0.24	0.16
S4 Gypsum Board	∞	89	45	∞	0.5	-0.38	-2.35
S5 PVC Covering on Gypsum Board	611	27	27	22.63	1.02	0.67	-0.3
S6 Paper Wall Covering on Gypsum Board	640	68	70	9.41	1.03	0.02	-0.95
S7 Textile Covering on Gypsum Board	639	72	20	8.88	0.28	3.16	-0.46
S8 Textile Covering on Mineral Wool	43	21	21	2.05	1.01	3.37	2.37
S9 Melamine Covering on Particle Board	465	147	631	3.16	4.29	-0.05	-0.28
S10 Expanded Polystyrene (PS)	115	85	41	1.35	0.49	6.76	4.71
S11 Polyurethane Foam (rigid)	6	4	68	1.5	17.09	1.05	0.99
S12 Wood Panel (Spruce)	131	66	1026	1.98	15.55	0.17	0.11
S13 Paper Covering on Particle Board	143	95	1076	1.51	11.33	-0.07	-0.16
E1 Painted Gypsum Paper on Plaster Board	∞	176	86	∞	0.49	-0.61	-2.67
E2 Ordinary Birch Plywood	160	116	804	1.38	6.93	-0.06	-0.21
E3 Textile Covering on Gypsum Board	670	111	80	6.04	0.72	0.19	-1.2
E4 Melamine faced High Density Non-Combustible Board	∞	102	130	∞	1.28	-0.46	-1.25
E5 Plastic faced Steel Sheet on Mineral Wool	∞	162	260	∞	1.61	-0.9	-1.53
E6 F.R. Particle Board Type B1	630	53	47	11.89	0.9	0.16	-0.95
E7 Combustible faced Mineral Wool	75	10	28	7.5	2.77	-0.39	-0.76
E8 F.R. Particle Board	∞	669	294	∞	0.44	-0.8	-3.08
E9 Polyurethane Foam on Plastic faced Steel Sheet	215	115	179	1.87	1.56	-0.05	-0.69
E10 PVC Wallcarpet on Gypsum Board	650	81	114	8.02	1.41	-0.04	-0.74
E11 Extruded Polystyrene Foam	80	80	48	1	0.6	3.16	1.49

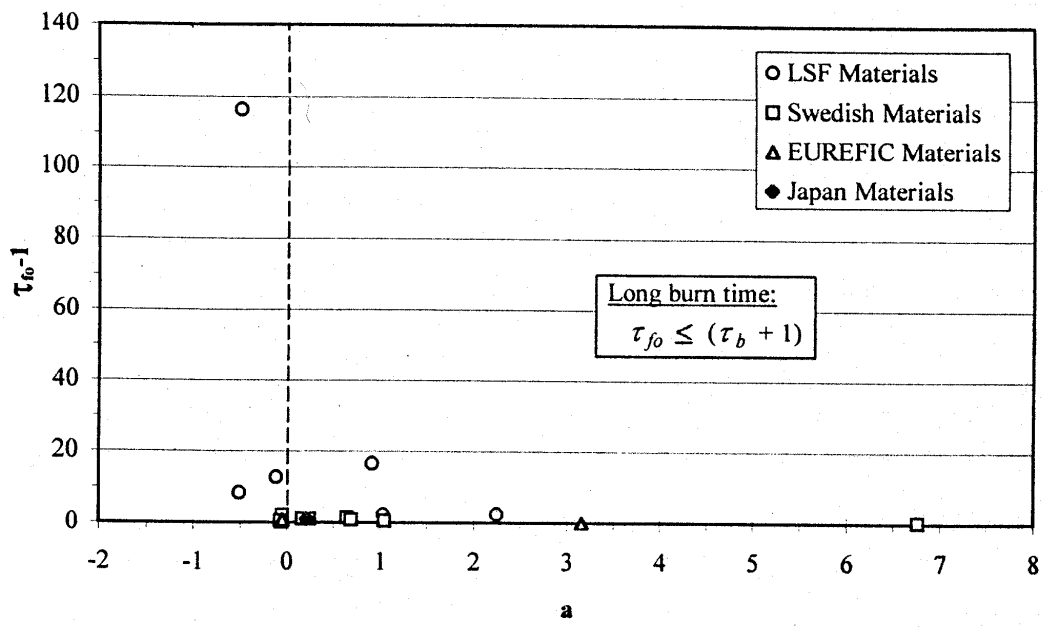

Figure 10. Correlation for flashover time before material burnout

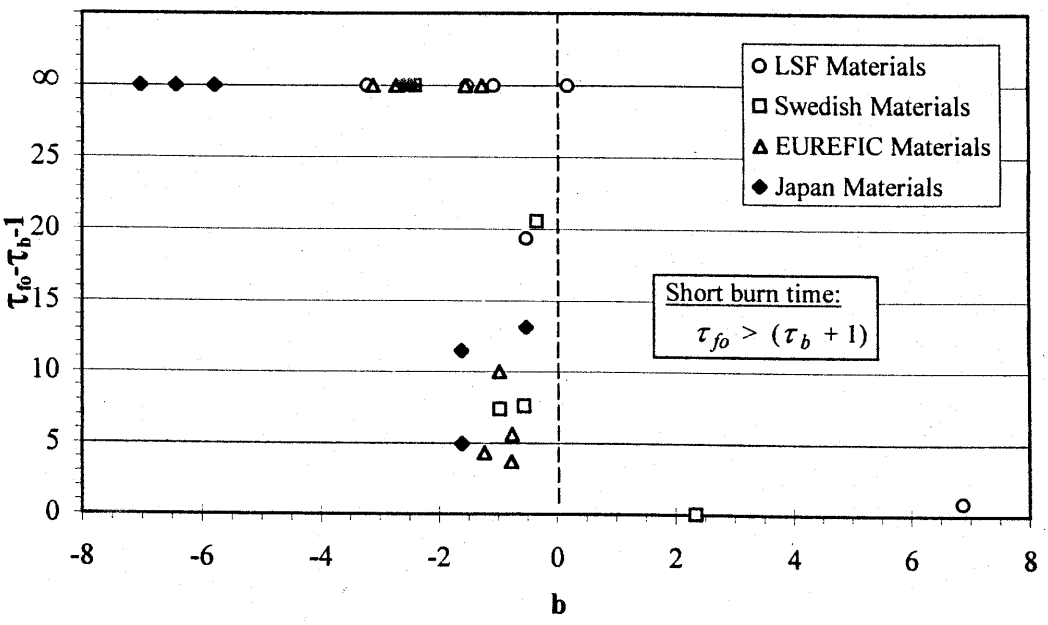

Figure 11. Correlation for flashover time after material burnout

rate relative to the initial value of the ignition source ($\dot{Q}_o''$):

$$\frac{\dot{Q}}{\dot{Q}_o} = \frac{(a+1)e^{a(t-1)}}{a} \quad \text{for } 0 \le t-1 \le t_b \text{ and}$$

$$\frac{\dot{Q}}{\dot{Q}_o} = ce^{b(t-1-t_b)} \text{ for } t-1 \ge t_b \qquad (9)$$

$$\text{with } c = \left(\frac{a+1}{a}\right)\left(e^{at_b}-1\right),\ a = k_f\dot{Q}'' - 1,\ b = a - 1/t_b$$

where t = t/t_{ig}, t_{ig} of Eq. (1),
t_b = t_b/t_{ig}, t_b of Eq. (8),
k_f = 0.01 m^2/kW,
and t is taken as zero at the exposure to the ignitor. This result shows that the energy release rate in upward spread is exponential in time. Furthermore, the exponent is controlled by a and b, and it can be positive or negative depending on the value of $\dot{Q}''$ and t_b. It suggests that for $\dot{Q}''$ < 100 kW/m^2 and for t_b comparable to the ignition time that spread may decelerate and cease.

This simple model has been used to correlate results for the ISO 9705 Room Corner Test. The test involves the corner exposure of a room lined with a material on the walls and ceiling to an ignition of 100 kW for 10 minutes, followed by 300 kW for another 10 minutes. The test is concluded if flashover (1 MW) occurs or at the end of the 20 minute ignition exposure. The flashover times have been examined for 45 materials, and the parameters a and b were computed from material properties and using a flame heat flux of 60 kW/m^2 in computing energy release rate and 30 kW/m^2 in computing t_{ig}. The material data to compute the properties were derived from several sources documented in Dillon (1998).

Table 1 lists the material properties for the data set associated with the 45 room corner tests. Table 2 lists experimental flashover times and the parameters from Eq. (9) used to examine the correlation for the flashover. As suggested by Eq. (9), two regions are examined: flashover before burnout considering the importance of the parameter, a, and after burnout considering b. The exponents involving time are the motivation of the plots in Figures 10 and 11 which correspond to the two regions. The results clearly show a distinct critical region for a and b between 0 and -2 which divides a region of no flashover for larger negative values from a region in which flashover time is more dependent on ignition time. These results seem to confirm the exponential character of upward spread which dominates the fire growth in the room corner test.

CONCLUSIONS

A rational procedure has been described to derive material properties from tests to serve the ability to compute aspects of fire growth. An example of the application of fire properties has been demonstrated in a correlation for 45 materials tested in the ISO room corner test. The correlation examines flashover time and shows the exponential nature of fire growth with respect to time.

ACKNOWLEDGEMENTS

Much of the raw data from Cone Calorimeter testing and the results of the ISO room corner test were supplied from the LSF Laboratories of Italy and the Building Research Institute of Japan. We are especially indebted to the efforts of Silvio Messa, Yuji Hasemi, and Yoshihiko Hayashi.

REFERENCES

ASTM E 1321, "Test Method for Determining Material Ignition and Flamer Spread Properties", 1996 Annual Book of ASTM Standards, Sec. 4, Vol. 04.07, ASTM, West Conshohocken, PA.

ASTM E 1354, "Test Method for Heat and Visible Smoke Release Rates for Materials and Products Using an Oxygen Consumption Calorimeter", 1996 Annual Book of ASTM Standards, Sec. 4, Vol. 04.07, ASTM, West Conshohocken, PA.

Cleary, T. G. and Quintiere, J. G., 1991, "A Framework for Utilizing Fire Property Tests", Fire Safety Science, Proceedings of the 3rd International Symp., ed. G. Cox and B. Langford, Elsevier Applied Science, London, pp. 647-656.

Dillon, S. E., 1998, "Analysis of the ISO 9705 Room/Corner Test: Simulations, Correlations and Heat Flux Measurements", M. S. Thesis, Department of Fire Protection Engineering, University of Maryland.

Long, R. T. Jr., 1998, "An Evaluation of the Lateral Ignition and Flame Spread Test for Material Flammability Assessment for Micro-gravity Environments", M. S. Thesis, Department of Fire Protection Engineering, University of Maryland.

Quintiere, J. G. and Harkleroad, M., 1984, "New Concepts for Measuring Flame Spread Properties", NBSIR 84-2943, Nat. Bur. Of Standards, Gaithersburg, MD.

Rhodes, B. T. and Quintiere, J. G., 1996, "Burning Rate and Flame Heat Flux for PMMA in a Cone Calorimeter", Fire Safety Journal, Vol. 26, No. 3, pp. 221-240.

Su, C-H, 1997, "Downward and Lateral Flame Spread in Roland Apparatus Phase 5", M.S. Scholarly Paper, Department of Fire Protection Engineering, University of Maryland.

Tewarson, A., 1988, "Generation of Heat and Chemical Compounds in Fires", SFPE Handbook of Fire Protection Engineering, Nat. Fire Prot. Assoc., Quincy, MA, pp. 1-179 to 1-199.

Wu, N. P., 1998, "Determination of Fire Properties of Liquid Fuels Characteristic of Oil Spills using ASTM E-1321, M. S. Thesis, Department of Fire Protection Engineering, University of Maryland.